Journal of
Applied Crystallography
ISSN 0021-8898

Received 12 August 2002
Accepted 27 January 2003

Analysis of the small-angle intensity scattered by a porous and granular medium

O. Spalla,* S. Lyonnard and F. Testard

CEA Saclay, DRECAM/SCM, Laboratoire Interdisciplinaire sur l'Organisation Nanométrique et Supramoléculaire, 91191 Gif sur Yvette, France. Correspondence e-mail: spalla@scm.saclay.cea.fr

Using X-ray scattering over a large range of scattering vectors, it is shown how to measure both the pore volume fraction and pore specific surface of an assembly of porous grains forming a powder. Depending on the presence or not of solvent in the inner pores and in the intergranular media, the scattered signal per unit volume of solid or per unit volume of grain are introduced, which allow a complete analysis even when the thickness of the layer and its compactness are unknown. The method is applied to three different systems presenting a well defined Porod regime at large scattering vector.

1. Introduction

Powders formed of porous grains of micrometric size are often encountered in materials science. The morphology of the grains, the total inner porosity available for ion adsorption, the size of the pores and their specific surface, have to be well characterized in view of further industrial applications. As an example, in the Synroc process for nuclear-waste disposal (Ringwood *et al.*, 1988), precursor nanoporous micrometric powders for producing advanced ceramics are prepared by spray-drying concentrated sols (Sizgek *et al.*, 1994). An experimental probe of the structure on the nanometre to the micrometre scale is of prime interest to optimize the chemical composition and refine engineering recipes to control the final morphology of the micro-grains and their porous properties.

Small-angle X-ray scattering (SAXS) has been shown for a long time to be a technique well suited to explore such systems and questions (Guinier & Fournet, 1955; Brumberger, 1965; Schaeffer *et al.*, 1995; Bale & Schmidt, 1984; Wong, 1985). Nevertheless, the collection of data in the correct unit (cm^{-1} for the scattered intensity I_{Abs} per unit volume of illuminated sample) requires one characteristic of the sample to be known: its thickness e_S. When manipulating inorganic powders of micrometric size, this conflicts with another general requirement, namely to make the sample very thin to avoid strong absorption and/or multiple scattering at small angle. For instance, when using a Cu $K\alpha$ source (8 keV) the sample is in general limited to a thin layer of grains of unknown thickness and solid content. Using an Mo source (or a synchroton) at 17.46 keV allows the examination of a sample of larger thickness (a few millimetres), but the solid content remains difficult to obtain with good accuracy.

In this paper, a new and general data analysis method is developed in order to avoid these difficulties. The experimental steps in data acquisition and treatment of this method are described in the first part of the paper. In the second part, an illustration is given using three materials: water-altered glass grains, spray-dried powders for Synroc, and mesoporous ceria.

2. Scattering by powders

2.1. General laws in small-angle scattering and position of the problem

SAXS is commonly used to determine the structure of materials in the colloidal domain. The intensity scattered by the sample is the Fourier transform of the spatial autocorrelation function, which contains information on the electronic density distribution. In general, SAXS 'absolute' (or scaled) intensity (cm^{-1}) in the direction $\mathbf{u}$ is defined as the differential scattering cross section $d\sigma(\mathbf{u})/d\Omega$ per unit volume V of illuminated sample and can be obtained from raw count rates by

$$I_{\rm Abs} = \frac{1}{V}\frac{d\sigma}{d\Omega}(\mathbf{u}) = \frac{C}{C_0 \Delta\Omega T e_S} \qquad (1)$$

where C_0 is the incoming flux of photons on the sample, C the number of photons collected per second in the solid angle $\Delta\Omega$, T the sample transmission, and e_S the sample macroscopic thickness. The first four quantities are known or measured during data collection, and depend on the experimental geometry.

When a sample of thickness e_S is homogenous on the macroscopic scale but contains two different phases with an electronic contrast $\Delta\rho$, two main quantities can be extracted from the scattered intensity: the volume fraction φ_S of one phase (taken to be the solid phase in the present case) and the total quantity of interface Σ (m^{-1}) between the two phases, *i.e.*

$$Q = \int_0^\infty I_{\rm Abs} q^2 \, dq = 2\pi^2 \varphi_S (1-\varphi_S)(\Delta\rho)^2, \qquad (2)$$

$$\Sigma = \left[\lim_{q\to\infty}(I_{\rm Abs} q^4)\right] \Big/ 2\pi(\Delta\rho)^2. \qquad (3)$$

Equation (3) is called the Porod limit (Porod, 1951, 1982) and is due to the presence of a well defined and smooth interface between the two phases. Note that a Porod limit is not always reached, especially in the case of rough interface (Bale &

Schmidt, 1984; Wong, 1985). The present work is restricted to systems presenting a Porod limit. Q is usually called the 'invariant' (Porod, 1982). When a wide q range is available, and provided that a correct (cm^{-1}) scaling of the intensity is achieved, the relevant parameters Σ and φ_S can be directly derived from these two equations. This is the case for dispersions of sub-micrometric particles in liquid for instance, where the sample macroscopic thickness e_S is easily measured and scaled intensities are routinely obtained.

Nevertheless, when considering a disordered assembly of porous grains, the measurement of the sample thickness is often impossible as very thin samples (<100 µm with a Cu source) are required to avoid strong absorption. The powders have to be deposited onto the surface of a Kapton sheet, thus forming a thin layer of grains: no precise macroscopic measurement of e_S is possible. Consequently, no true absolute intensity can be extracted. When using harder X-rays (an Mo source for instance), the powders can be kept between two Kapton sheets, and typical cells of 0.5 mm can be used, but one has to ensure that the data are not corrupted by multiple scattering at low angle. In the case of a thick sample, the compactness of the powder is in general unknown.

As a consequence of these difficulties with sample handling, it is important to understand that even if the sample specific surface Σ is obtained, this value is not relevant because it is scaled by the volume of sample and not by the volume of solid. The absolute intensity per unit volume of sample being unreachable in general with powders, another way of treating the raw data C (counts s^{-1}) is required, which does not require the measurement of the thickness e_S and allows one to reach quantities ascribed to the unit volume of the solid. In proposing such a method, we will start by considering in detail the geometry of a porous and granular medium.

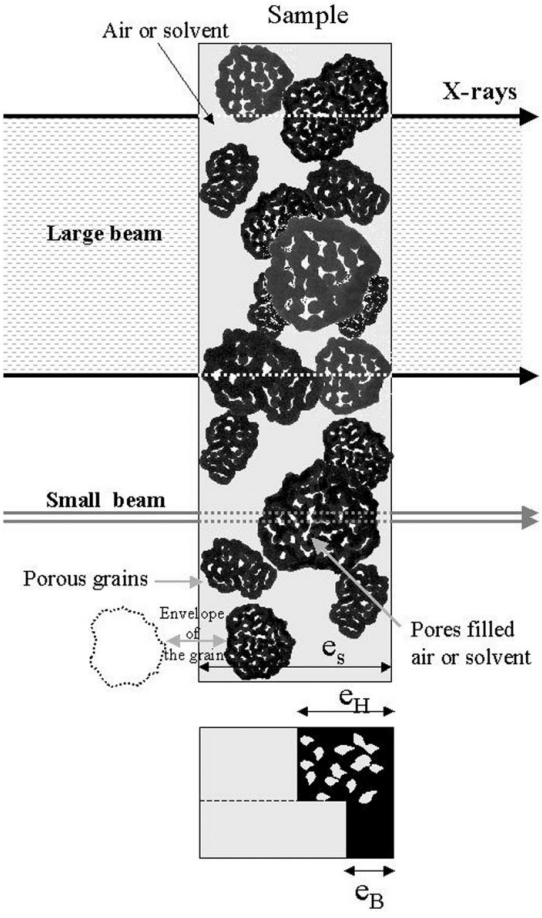

Figure 1
Sample configuration in a section parallel to the beam. A volume fraction φ^* of porous grains is either deposited onto one Kapton sheet, or kept between two Kapton sheets as shown here. The macroscopic thickness is e_S. The porous volume fraction inside each grain is φ, such that the total porous fraction is $\varphi\varphi^*$. The equivalent solid thickness e_B and equivalent grain (solid + inner pores) thickness e_H are also defined.

2.2. Powder porosity and compactness

Fig. 1 shows a schematic view of a typical sample section parallel to the beam. Obviously, the granular medium does not fill the whole cell. A compactness φ^* of the sample can be defined as the ratio between the total volume of the envelopes of the grains V_e divided by the volume of the sample V:

$$\varphi^* = V_e/V. \tag{4}$$

It has to be noted that the definition of the 'envelope' of a grain is not always straightforward. Nevertheless, it can be easily done when the system presents two length scales: nanopores (or particles) of a few nanometres in diameter on the one hand, inserted in micrometric grains on the other hand. In that case, an outer envelope of the grain can be defined by smoothing the external border of the grain. This smoothing is not relevant when the pores size and grain size are in the same range. We now consider the total volume of pore V_i contained in the total volume of the grain envelope and define an inner porosity φ by

$$\varphi = V_i/V_e. \tag{5}$$

Reciprocally, the volume of solid V_s is related to V_e by

$$V_s/V_e = 1 - \varphi. \tag{6}$$

The solid volume fraction φ_S of the sample is therefore simply related to φ^* and φ by

$$\varphi_S = \varphi^*(1 - \varphi). \tag{7}$$

The inner porosity φ is an intrinsic property of the material whereas the solid volume fraction of the sample φ_S depends on the compactness. Therefore, φ is one of the major properties that have to be deduced from the scattering data.

The illuminated sample presents a specific surface Σ that arises mainly from the inner porosity of the grains in the case in which the pores are much smaller than the grains. The total amount of interface of the grains is denoted S and the total amount of envelope surface of the grains is denoted S_e. S counts the total interface of the grain including the inner porous surface and the true outer interface. Therefore, it has a clear and unambiguous definition. On the other hand, S_e results from a smoothing of the outer shape of the grain and is relevant only when the notion of envelope is relevant.

The porous and envelope surfaces can be scaled by the volume of the sample through

$$\Sigma = S/V \tag{8}$$

and

$$\Sigma_e = S_e/V. \tag{9}$$

In the case under study, one has $\Sigma \gg \Sigma_e$. Nevertheless, the two specific surfaces Σ and Σ_e per unit volume of sample are useless because the compactness φ^* of the sample is unknown. It is much more relevant to scale them by the solid phase volume V_s:

$$\Sigma_S = S/V_s = \Sigma/\varphi^*(1-\varphi) \tag{10}$$

and

$$\Sigma_{e,S} = S_e/V_s = \Sigma_e/\varphi^*(1-\varphi), \tag{11}$$

or by the envelope volume V_e of the grains:

$$\Sigma_G = S/V_e = \Sigma/\varphi^* \tag{12}$$

and

$$\Sigma_{e,G} = S_e/V_e = \Sigma_e/\varphi^*. \tag{13}$$

The three quantities which are of interest to characterize the porous and granular media are indeed Σ_S, φ and $\Sigma_{e,G}$. The aim of this paper is to show how they can be extracted directly from the raw signal using relations derived from the general laws [equations (2) and (3)] in the special case of powders.

The proposed method is based on the introduction of a so-called 'measurable intensity' when the compactness φ^* and/or the thickness e_S of the sample are unknown.

2.3. Measurable intensities

Depending on the pre-treatment of the powders, three main situations can be encountered: air inside the inner pores and in the inter-grains porosity, solvent solely inside the inner pores and air in the inter-grain porosity, and finally solvent everywhere. These three situations are treated successively. The scattering length density of the solid is denoted ρ and its absorption coefficient $\mu_{\rm solid}$. The solvent has a scattering length density denoted ρ_s and an absorption coefficient noted $\mu_{\rm solvent}$.

2.3.1. Case (i): air in the inner pores and the inter-grains porosity. The macroscopic thickness is not accessible. Nevertheless, an apparent thickness e_B can be calculated from transmission measured as the ratio of the beam flux transmitted by the sample divided by the flux transmitted by the empty cell:

$$e_B = -\ln(T)/\mu_{\rm Solid}. \tag{14}$$

The absorption coefficient $\mu_{\rm Solid}$ is calculated from the composition of the dry powder. e_B represents the average solid thickness on the path of the X-ray beam as shown in Fig. 1 and is related to the sample thickness e_S by

$$e_B = e_S\varphi^*(1-\varphi). \tag{15}$$

The 'measurable' intensity that can be extracted from the experimental data is therefore

$$I_1 = C/C_0\Delta\Omega T e_B. \tag{16}$$

2.3.2. Case (ii): solvent in the inner pores and air in the inter-grains porosity. The thickness is again not easily measured. Nevertheless, an apparent thickness e_H can be calculated from the transmission T using $e_H = -\ln(T)/\mu_{\rm Grain}$ provided that the absorption coefficient is correctly calculated. The thickness e_H is linked to the thickness of the sample by

$$e_H = e_S\varphi^*. \tag{17}$$

e_H is the average thickness of material (solid + inner pore) on the path of the X-ray beam as shown in Fig. 1. The absorption coefficient $\mu_{\rm Grain}$ is calculated from the composition of the powder:

$$\mu_{\rm Grain} = \mu_{\rm Solid}(1-\varphi) + \mu_{\rm Solvent}\varphi, \tag{18}$$

where we assume that the solid skeleton is homogeneous. Two remarks have to be made at this stage. Firstly, the two thicknesses e_B and e_H are not equal even if the pores are empty of solvent. Secondly, as the calculation of $\mu_{\rm Grain}$ uses the volume fraction φ of pores, a consistency test is obtained by comparing the assumed initial φ used to calculate $\mu_{\rm Grain}$ with the final determination of φ from the invariant (see end of §3.1). The procedure can be cycled until consistency is obtained. The measurable intensity that can be calculated from the experimental data is therefore

$$I_2 = C/C_0\Delta\Omega T e_H. \tag{19}$$

2.3.3. Case (ii): solvent in the inner and inter-grains porosity. When the sample can be made thick enough by dilution (for instance in a solvent containing a slight amount of xanthan gum to suspend the grains), the thickness can be measured correctly. Therefore, this is a situation where the absolute intensity $I_{\rm Abs}$ per unit volume of the sample is measurable. The mass fraction of grains can be measured by precisely weighing a large amount of the paste from which the sample is extracted before and after drying at 373 K. Then, knowing the density of the materials, the volume fraction of solid $\varphi_S = \varphi^*(1-\varphi)$ can be deduced.

Nevertheless, the weighing method works well only when the 'paste' is homogeneous with respect to the size of the beam. When the incident beam is very small (a few 100 µm), another solution is to deduce the volume fraction of solid from the transmission of the sample. Indeed, the transmission of the wet paste is

$$T = \exp(-\mu_{\rm Paste}e_S) \ \text{ with } \ \mu_{\rm Paste} = \varphi_S\mu_{\rm Solid} + (1-\varphi_S)\mu_{\rm Solvent}, \tag{20}$$

where $\mu_{\rm Solid}$ is calculated from the composition of the solid. In that case, $\mu_{\rm Paste}$, $\mu_{\rm Solid}$ and $\mu_{\rm Solvent}$ have to be known in order to calculate φ_S. Finally one can scale the intensity to the solid content like in case (i):

$$I_1 = I_{\rm Abs}/\varphi_S. \quad (21)$$

2.4. Experimental

A correct measurement of the scattered intensity requires a very large range of scattering vector, typically from 3×10^{-4} Å^{-1} to 1 Å^{-1}. This is in general available only by coupling different setups as described in this experimental section. In the laboratory, SAXS experiments have been performed either on a conventional two-dimensional Guinier camera or a Huxley–Holmes camera. The Guinier camera (Né *et al.*, 2000) is installed on an Mo source delivering high-energy photons (λ = 0.71 Å). The Huxley–Holmes camera (Zemb *et al.*, 2003) is installed on a rotating anode with a Cu target. The scattering intensities can be detected in the range from 0.01 to 1 Å^{-1}. USAXS experiments have been performed on a one-dimensional camera with two Ge channel-cut crystals in Bonse–Hart geometry. The performance of this instrument has been described elsewhere (Lambard *et al.*, 1992). The available q range is complementary to that of the Guinier camera: from 3×10^{-4} to 0.1 Å^{-1}. The detection system is composed of an analyser crystal and a photomultiplier counter under vacuum. The horizontal resolution function, the so-called rocking curve, is obtained by measuring the intensity without a sample. Its FWHM is 80 µrad, *i.e.* 3×10^{-4} Å^{-1}. The machine is installed on a rotating Cu anode delivering photons at λ = 1.54 Å. As the vertical geometry of the machine is linear, data need to be desmeared. Combining the two spectrometers allows a q range extending over four decades to be covered, which means that one measurement can give information about heterogeneities in the sample ranging from a few ångströms to a few micrometres. The technique is thus particularly well adapted when the observation of a material on two different length scales is needed.

For both setups, the 'measurable' scaled intensities I_1 or I_2 are obtained by controlling the sample transmission, the solid angle of the experiment, and the incoming flux (Lambard *et al.*, 1992; Zemb *et al.*, 2003; Né *et al.*, 2000) and the use of secondary standards is not required. The true scaled intensity $I_{\rm Abs}$ is obtained only when the sample thickness can be measured. All the data are background subtracted (to eliminate scattering due to solvent, for instance). Finally, it has to be noted that the beam in the three setups is a few mm^2 wide at the sample position. The USAXS spectra have been desmeared by Strobl's method (Strobl, 1970).

Some experiments were also performed on beamline BM02 (French CRG) at the ESRF in Grenoble. A large q range was obtained using two different sample–detector distances. The absolute or 'measurable' intensities were registered by controlling the sample transmission, the solid angle of the experiment, and the incoming flux in both distances.

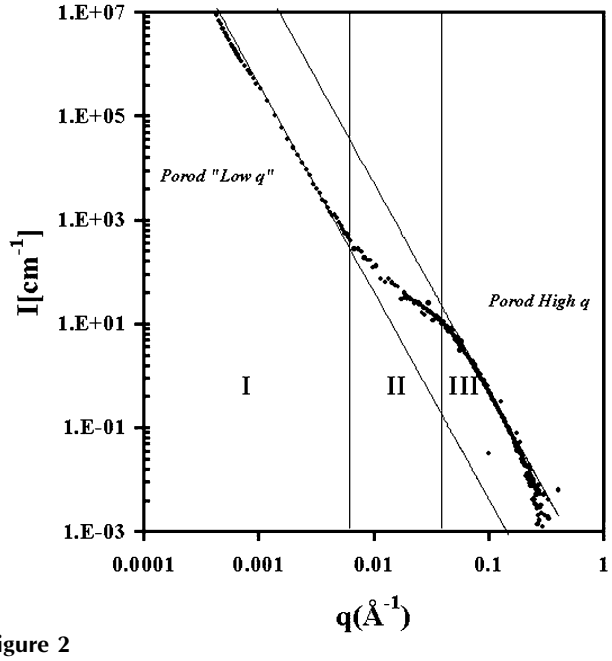

Figure 2
Typical apparent intensity of a two-length-scale porous system (water-altered glass). Three regions are identified: (I) a low-q Porod's law region; (II) an intermediate plateau; (III) a high-q Porod's law region.

3. Model for data treatment

A typical measured signal is shown in Fig. 2. Three different regimes are observed: (I) a Porod regime at low q values due to the envelope of the grains; (II) a transition regime between; (III) a second Porod regime at high q values due to the inner pores of the grains.

3.1. Determination of φ by the invariant Q

The analysis starts by rearranging the granular layer in a double layer: one layer containing the material, of thickness e_H and inner porosity φ (named the 'material layer'), and one of thickness $e_s - e_H$ containing only solvent or air. During this step, the only scattering which disappears is that in the low-q limit, which corresponds to the outer envelope of the grain. This point is discussed in more detail at the end of §3.4. Hence, we define

$$I_{\rm Abs}^{\rm Corr} = I_{\rm Abs} - I_{\rm Abs}(q_*)q_*^4/q^4. \quad (22)$$

Using the definition of I_1 and I_2 one obtains

$$I_1^{\rm Corr} = I_{\rm Abs}^{\rm Corr}/\varphi^*(1-\varphi) \quad (23a)$$

and

$$I_2^{\rm Corr} = I_{\rm Abs}^{\rm Corr}/\varphi^*, \quad (23b)$$

where q_* is any value of q in the region (I). By construction, $I_1^{\rm Corr}$ and $I_2^{\rm Corr}$ are defined only in region (II) and (III). It is easy to show that the absolute intensity of the 'material layer' is equal to

$$I_{\rm Abs,mat} = I_{\rm Abs}^{\rm Corr}/\varphi^*. \quad (24)$$

Thus, the intensity scattered by the equivalent homogenous 'material layer' is experimentally accessible only in the regions (II) and (III) of scattering vectors. The equation (2) is directly applicable for the 'material layer' because it is homogenous with a volume fraction of pores φ:

$$\int_0^\infty I_{\mathrm{Abs,mat}} q^2 \, \mathrm{d}q = 2\pi^2 \varphi(1-\varphi)\Delta\rho^2, \tag{25}$$

with $\Delta\rho = \rho$ for case (i) (§2.3.1) and $\Delta\rho = \rho - \rho_s$ for cases (ii) and (iii) (§§2.3.2 and 2.3.3).

Finally coupling, equations (23), (24) and (25), cases (i) and (iii) yield

$$\int_0^\infty I_1^{\mathrm{Corr}} q^2 \, \mathrm{d}q = 2\pi^2 \varphi \Delta\rho^2, \tag{26a}$$

while for case (ii)

$$\int_0^\infty I_2^{\mathrm{Corr}} q^2 \, \mathrm{d}q = 2\pi^2 \varphi(1-\varphi)\Delta\rho^2. \tag{26b}$$

Experimentally, the calculation of the integral in the left side of equations (26) requires an extrapolation of I_1^{Corr} and I_2^{Corr} in the region (I) of scattering vector where they cannot be accessed experimentally. We assume a constant value in this region, equal to the first significant value for the lowest q in region (II). We can thus access φ directly from the measurable intensities I_1 or I_2 depending on the physical case [without knowing the compactness φ^* and the real thickness of the sample in cases (i) and (ii)], provided that the electronic densities of the material and solvent are known, and the transmission is measured properly.

The choice between I_1 and I_2 to treat the raw data, depends whether one considers case (i) or (ii) to be appropriate after a detailed examination of the history of the powder. In the case (ii), where solvent is supposed to be present inside the inner pore of the grain, the equation (26*b*) yields a final value which has to be consistent with that supposed in equation (18) used to calculate the adsorption of the composite wet grain. The procedure has in general to be cycled until the consistency is reached.

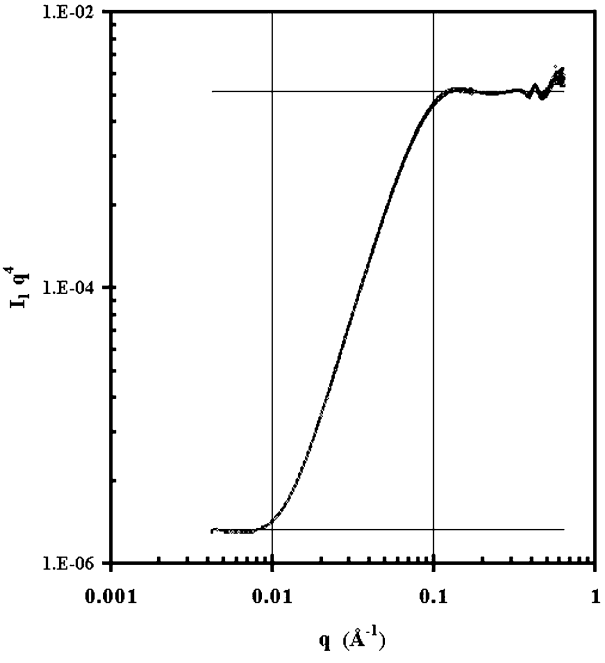

Figure 3
Porod representation $I_1 q^4$ *versus* q of the intensity for an altered grain. The asymptotic limits at large and small angles are evidenced.

3.2. Determination of the specific surface of pores from high-*q* Porod law

The asymptotic limit of Porod's law can be obtained by plotting the intensity in Porod's representation, *i.e.* Iq^4 as a function of q, as shown in Fig. 3. In the high-q domain, the specific surface corresponds to the interface between pores and bulk material. Using equations (3) and (10) one obtains for cases (i) and (iii)

$$\Sigma_S = \frac{1}{\varphi^*(1-\varphi)} \frac{\lim_{q\to\infty}(I_{\mathrm{Abs}} q^4)}{2\pi\Delta\rho^2} = \frac{\lim_{q\to\infty}(I_1 q^4)}{2\pi\Delta\rho^2}, \tag{27}$$

and for case (ii)

$$\Sigma_G = \frac{1}{\varphi^*} \frac{\lim_{q\to\infty}(I_{\mathrm{Abs}} q^4)}{2\pi\Delta\rho^2} = \frac{\lim_{q\to\infty}(I_2 q^4)}{2\pi\Delta\rho^2}, \tag{28}$$

where again I_1 and I_2 are directly measurable. The results are obtained in m^{-1}. Nevertheless, a specific surface is often expressed in $\mathrm{m}^2\,\mathrm{g}^{-1}$. To do so one has simply to divide the above formulae by the density of the solid d_m ($\mathrm{g\,m}^{-3}$). Note that in the examples which will follow (§4), this will be done automatically without changing the notations of Σ_S and Σ_G.

3.3. Determination of S_e/V_e from low-q Porod law

The same method is applied to the low-q Porod regime, where the scattering arises from the contrast $\Delta\rho^*$ between air or solvent and grains: $\Delta\rho^* = (1-\varphi)\rho$ for case (i), $\Delta\rho^* = (1-\varphi)\rho + \varphi\rho_s$ for the case (ii), and $\Delta\rho^* = (1-\varphi)(\rho - \rho_s)$ for case (iii). For the three different cases, (i), (ii) and (iii), the use of equations (3) and (13) respectively yields

$$\Sigma_{e,G} = \frac{1}{\varphi^*} \frac{\lim_{q\to 0}(I_{\mathrm{Abs}} q^4)}{2\pi\Delta\rho^2} = \frac{\lim_{q\to 0}(I_1 q^4)}{2\pi\rho^2(1-\varphi)}, \tag{29}$$

$$\Sigma_{e,G} = \frac{1}{\varphi^*} \frac{\lim_{q\to 0}(I_{\mathrm{Abs}} q^4)}{2\pi\Delta\rho^2} = \frac{\lim_{q\to 0}(I_2 q^4)}{2\pi\Delta\rho^{*2}}, \tag{30}$$

$$\Sigma_{e,G} = \frac{1}{\varphi^*} \frac{\lim_{q\to 0}(I_{\mathrm{Abs}} q^4)}{2\pi\Delta\rho^2} = \frac{\lim_{q\to 0}(I_1 q^4)}{2\pi(\rho-\rho_s)^2(1-\varphi)}. \tag{31}$$

3.4. Scattering by a porous grain

The above formulae do not suppose anything about the geometric repartition of the porous surface inside the grains but that the grain is homogeneously porous. In this section, we use a model that supposes the grains to be all identical and globular with a volume V, each containing n pores of volume v. The scattering intensity is the Fourier transform of the correlation function between two elementary volumes i and j located in the complementary region of the solid. Three contributions can be separated as follow.

First, i and j are located outside the grain envelope. The scattering intensity is

$$I_a = (\rho_{out} - \rho)^2 V^2 F_0^2(q) = (\rho_{out} - \rho)^2 V^2 P_0(q), \quad (32)$$

where ρ_{out} is the scattering length density in the inter-grain porosity, $F_0(q)$ the amplitude and $P_0(q)$ the normalized intensity of the form factor of an homogeneous grain.

Second, i and j are located inside the grain. The scattered intensity is

$$I_b = (\rho - \rho_{in})^2 n v^2 f_0^2(q)[S(q) + (n-1)P_0(q)], \quad (33)$$

where ρ_{in} is the scattering length density inside the pore, $f_0(q)$ the normalized amplitude scattered by a pore and $S(q)$ the structure factor of pores.

Third, i is inside, while j is outside the grain envelope. The scattered intensity is

$$I_c = -2(\rho_{out} - \rho)(\rho_{in} - \rho) n v V P_0(q) f_0(q). \quad (34)$$

The global intensity is the sum of the three contributions. Taking N grains with a macroscopic volume fraction φ^*, and considering the case of uncorrelated pores [$S(q)$ equal to 1 at each q] the final absolute intensity becomes

$$I_{Abs} = \varphi^* \{\varphi v f_0^2 (\rho - \rho_{in})^2 + V P_0[(\rho - \rho_{out})^2 - 2\varphi f_0 (\rho_{out} - \rho)(\rho_{in} - \rho) + \varphi^2 f_0^2 (\rho - \rho_{in})^2]\}. \quad (35)$$

The two Porod limits in three different cases are recovered by equation (35) without any approximation. On the other hand, the approximation made in the determination of the invariant [left side of equation (25)] can be discussed. Indeed, from equation (35) the dominant term when q tends to 0 is

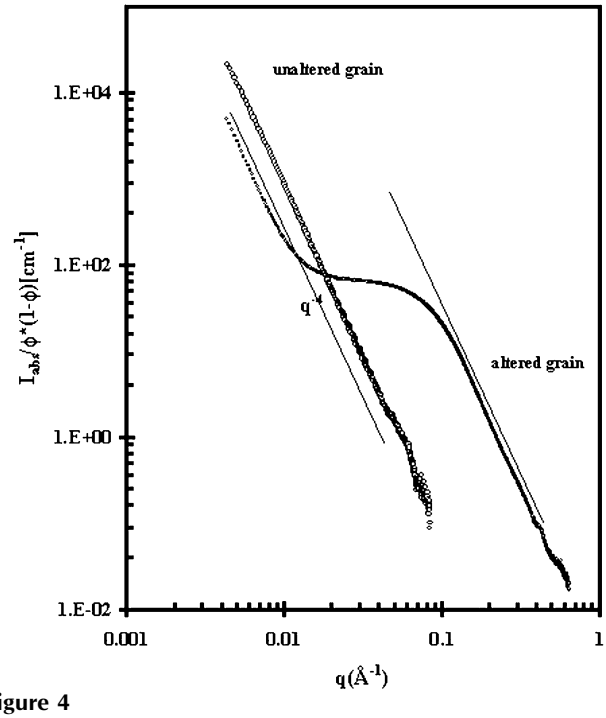

Figure 4
Scattering diagrams of glass grains (average size 20 μm), normalized to the total solid quantity per unit volume $I_{abs}/[\varphi^*(1-\varphi)]$. When the grain is unaltered, a pure Porod limit is observed, while a porous structure is revealed at large angle when the grains have been altered.

$$I_{Abs} = \varphi^* V P_0[(\rho - \rho_{out})^2 - 2\varphi(\rho_{out} - \rho)(\rho_{in} - \rho) + \varphi^2(\rho - \rho_{in})^2], \quad (36)$$

since f_0 is equal to 1 in region (I). Therefore, coupling equations (22), (23), (24), (35) and (36), one obtains

$$I_{Abs,mat} = \varphi v f_0^2 (\rho - \rho_{in})^2 + V P_0[-2\varphi(f_0 - 1)(\rho_{out} - \rho)(\rho_{in} - \rho) + \varphi^2(f_0^2 - 1)(\rho - \rho_{in})^2] \quad (37)$$

When calculating the invariant Q of the material layer, the first term in equation (37) leads to equation (25) and the others yield a correction which can be neglected as long as the ratio of size between the grain and the pores is high enough (more than 10). Indeed, in that case, P_0 is negligible in regions (II) and (III), which constitute the main contribution of the invariant Q. This quantifies the approximation made during the rearrangement of the granular layer in a bilayer (material + air) in §3.1 for the calculation of the inner porosity φ.

4. Examples of application

The inner porosity of a grain is a relevant characteristic in several fields of materials science. We present below three examples where the X-ray measurements have provided direct information on the system: water-altered glasses [case (i)], spray-dried Synroc powders [case (ii)] and mesoporous ceria [case (iii)].

4.1. Water-altered glasses

Glass grains can be altered in hot water, with kinetics depending on the glass composition and the surrounding solution. This process is relevant, for instance, to glass fibres, which have to dissolve rapidly when accidentally inhaled. For glass grains of a few micrometres of (molar composition) SiO_2/Na_2O/B_2O_3/ZrO_2 = 70/14/14/2, after only one month of contact at 363 K, the surrounding water contains all of the B and Na. This shows that the residual glass grains are altered down to the centre and are made of Si, Zr and O. The question is to determine the volume fraction φ of pores and the specific surface Σ_S of the final product.

It is important to work *in situ* in order to avoid a corruption of the result by capillary forces. Accordingly, the glass grains (either altered or not) were suspended in a dilute xanthan solution, which formed a gel. The study was performed on beamline BM02 at the ESRF with a thin beam (300 × 300 μm) of energy 17.7 keV. Therefore, the effective volume fraction of solid φ_S cannot be well determined by weighting a macroscopic replica of sample because the paste can be locally heterogeneous on the lateral extension of the beam. The sample thickness was 2 mm. Using equation (20), the solid content φ_S on the path of the beam can be deduced using the measured transmission.

The diagrams of scattering before and after alteration are shown together in Fig. 4. A procedure of type (iii) is applied. Before the alteration, a pure Porod regime is obtained in the whole range of q. Therefore, the specific surface of the initial powder can be determined using equation (31) applied with φ

= 0, the solid fraction φ_S being calculated through the transmission of the sample $T = 0.556$ (at 17.7 keV). The thickness of the cell was 2 mm and therefore the paste has an absorption coefficient of $\mu_{\rm Paste} = 2.9\ {\rm cm}^{-1}$. The dry powder has a measured density of $d = 2.68\ {\rm g\ cm}^{-3}$, and its absorption coefficient at 17.7 keV is $\mu_{\rm Solid\text{-}Unaltered} = 9.19\ {\rm cm}^{-1}$. For water, $\mu_{\rm Solvent} = 1.16\ {\rm cm}^{-1}$ and the volume fraction of solid φ_S is found to be 0.22. Finally, taking a scattering length density contrast $\Delta\rho$ between the glass and water of $2.17 \times 10^{11} - 9.3 \times 10^{10} = 1.24 \times 10^{11}\ {\rm cm}^{-2}$, the specific surface of the 'grains' amounts to $\Sigma_{e,G} = 8.65 \times 10^5\ {\rm m}^{-1}$. The density of the pristine glass being 2.68 g cm^{-3}, the specific surface is thus 0.32 m^2 g^{-1}. This result is in good agreement with a BET measurement: 0.3 m^2 g^{-1}.

The same procedure has been used for the diagram of altered grains, which was also presented in a Porod plot (Iq^4 *versus* q) in Fig. 3. The transmission was equal to 0.446, yielding a sample absorption of $\mu_{\rm Paste} = 4\ {\rm cm}^{-1}$ and a volume fraction of $\varphi_S = 0.40$ (the absorption of the solid taking into account the leaching of some elements: $\mu_{\rm Solid\text{-}Altered} = 8.26\ {\rm cm}^{-1}$). In order to calculate properly the invariant Q from the diagram, the corrected intensity $I_{\rm Abs}^{\rm Corr}$ has been extended by a Porod law for the q range above the maximum experimental q vector, and a constant value below $q_{\rm min}$. The last unknown parameter is the scattering length density contrast $\Delta\rho$ between the residual skeleton and the water in the pore. One option is to take it as equal to the value for the pure initial glass ($1.24 \times 10^{11}\ {\rm cm}^{-2}$). Using equations (26*a*), (27) and (31), this leads to $\rho = 2.17 \times 10^{11}\ {\rm cm}^{-2}$, $\varphi = 0.175$, $\Sigma_S = 119\ {\rm m}^2\ {\rm g}^{-1}$, $\Sigma_{e,G} = 4.27 \times 10^5\ {\rm m}^{-1}$.

The decrease of the value of $\Sigma_{e,G}$ (external envelope of the grain) would mean that the size of the grain has increased by a factor of more than two, which seems unrealistic. A more reasonable option is that the skeleton electron density has slightly decreased. It can be adjusted in order to recover the correct envelope specific surface, $\rho = 1.95 \times 10^{11}\ {\rm cm}^{-2}$, $\varphi = 0.26$, $\Sigma_S = 158\ {\rm m}^2\ {\rm g}^{-1}$, $\Sigma_{e,G} = 8.6 \times 10^5\ {\rm m}^{-1}$.

The value for the skeleton remains close to that of quartz silica. An interesting comparison can be made with the chemical titration. Indeed, it was found that all the B and Na atoms have been leached from the grain. If it is assumed (as done classically) that the volume left by their departure is dominated by the volume of the oxygen atoms bound to them in an oxide form, one arrives at a 'chemical volume fraction' of $\varphi_{\rm ch} = 0.28$, close to the X-ray determined value.

A second example is given where the normalization is done by weighting the sample. The glass composition is $SiO_2/Na_2O/B_2O_3 = 54/17/29$ (molar fraction), such that the surrounding water contains all of the B and Na after only one week of alteration at 363 K with a surface of solid to volume of solution ratio of 20 cm^{-1}. After the alteration, the grains were suspended in a dilute xanthan solution, which formed a gel. The volume fraction of solid, determined by weighing the sample before and after drying at 373 K, was $\varphi_S = 0.018$. Note that, as the residual solid is pure silica, with an absorption coefficient of $\mu_{\rm Solid}(8\ {\rm keV}) = 79\ {\rm cm}^{-1}$, taking the absorption coefficient of water equal to $\mu_{\rm Solvent}$ (8 keV) = 10.7 cm^{-1}, the absorption coefficient of the paste amounts to $\mu_{\rm Paste}(8\ {\rm keV}) = 12\ {\rm cm}^{-1}$. The thickness of the sample is 1 mm, which yields a transmission of $T = 0.88$ as compared to pure solvent. Hence, for that weak amount of solid, the procedure using the transmission requires a very precise measurement of the transmission. The scattering diagram of the grains after alteration is shown in Fig. 2.

A procedure of type (iii) has again been applied to the collected data. In order to calculate properly the invariant Q, the corrected intensity $I_{1,\rm corr}$ has been extended by a Porod law for the q range above the maximum experimental q vector. The pore volume fraction φ is found to be 0.34 and the inner specific surface can be deduced: $\Sigma_S = 145\ {\rm m}^2\ {\rm g}^{-1}$, yielding a pore radius of 4.3 nm, assuming a spherical shape and using the relation

$$r = 3\rho_m(1-\varphi)/\Sigma_S\varphi, \tag{38}$$

where ρ_m is the volume mass of the solid's skeleton. Furthermore, the surface/volume of the grains is now $\Sigma_{e,G} = 1.8\ {\rm m}^2\ {\rm g}^{-1}$. This means that the initial grains have been fragmented by the alteration process. Accordingly, the process of alteration of that sort of grain far above the percolation threshold can be described as follows: they are fragmented in around 100 pieces, which are themselves altered down to the centre with a volume fraction of 34% and pores of a few nanometres size.

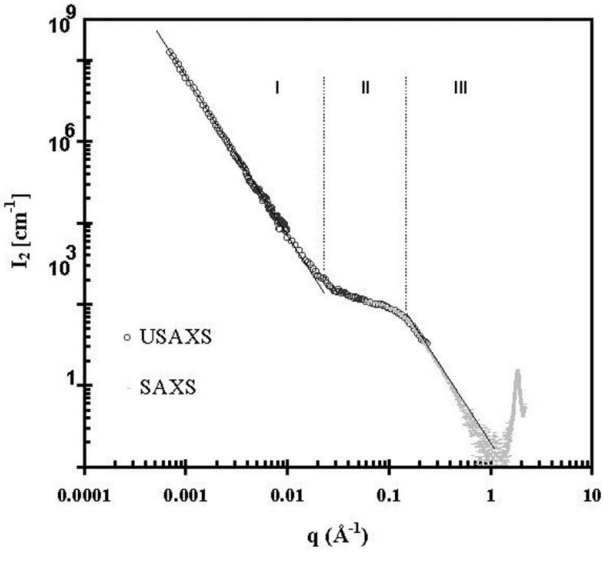

Figure 5
Apparent intensity I_2 of a TiO_2 powder (from a stock suspension of $[TiO_2] = 500\ {\rm g\ l}^{-1}$, and 0.15 M salt) on SAXS (grey dots) and USAXS (black circles). The anatase Bragg peak ⟨101⟩ is observed at high q.

4.2. Spray-dried powders for Synroc

Precursor powders used in the Synroc process for nuclear-waste storage are produced by spray-drying concentrated solutions of TiO_2 nanoparticles synthesized in nitric acid. The fast drying of fine droplets of the sol (20 to 50 µm) leads to the formation of porous microspheres (Lyonnard *et al.*, 2002). The

Table 1
Electronic contrasts of a titania powder when considering pores filled by water (model 1), water and electrolyte (model 2), water + electrolyte + nitric acid (model 3), water + nitric acid (model 4).

By the comparison between $\Delta\rho$ obtained from sample composition and $\Delta\rho_{\text{X-rays}}$ derived from our analysis, models 2, 3 and 4 have been rejected.

Sample	Model 1	Model 2	Model 3	Model 4
$\Delta\rho_{\text{calc}}$ ($\times 10^{11}$ cm^{-2})	2	1.8	2.03	1.88
$\Delta\rho_{\text{X-rays}}$ ($\times 10^{11}$ cm^{-2})	1.98	1.95	1.93	1.92

Table 2
Physical parameters obtained from SAXS analysis compared with N_2 sorption (BET) and SEM (volume fraction, specific surface of the pores, radius of the pores, radius of the grains).

φ		Σ_S (m^2 g^{-1})		r (nm)		R (μm) = $3V_e/S_e$	
SAXS	N_2 sorption	SAXS	N_2 sorption	SAXS	BJH	SAXS	SEM
0.37	0.29	340	298	1.4	1.3	5.6	6.5

final morphology of these micrometric grains (20 μm), as well as the specific surface and the total porosity, which are of prime interest for further ion adsorption, strongly depend on the initial sol and electrolyte [$Al(NO_3)_3$] concentration. It has been showed that in the absence of salt, an aerosol is produced (fragmentation is favoured instead of compaction) while 0.15 *M* of electrolyte optimizes the compaction mechanism and leads to well defined spherical grains with up to ∼30% porosity.

The powder appears dry. Nevertheless, infrared analysis has shown that the material contains water, the solid weight fraction being measured by weighting the sample before and after burning. The water volume fraction in the powder is found to be 0.37 for the typical sample presented below. The pores are consequently filled by fluid, and case (ii) of the porous scattering model has been applied to interpret the data. Very thin layers of powders were deposited on a sticky Kapton sheet. USAXS and SAXS intensities obtained on spray-dried powders prepared at different titania concentration, in the absence and in the presence of salt, all exhibit the two-Porod shape typical of hierarchical systems with two length scales and an internal porosity. As an example, Fig. 5 shows the measurable scattering intensity I_2 obtained for a TiO_2 powder prepared from a suspension of [TiO_2] = 500 g L^{-1}, with a molar ratio of 0.1 mole HNO_3 per mole of TiO_2, and [$Al(NO_3)_3$] = 0.15 *M*.

The main difficulty in this $TiO_2/HNO_3/Al(NO_3)_3/H_2O$ system arises from the chemical species of the pore fluid and the titania-based matrix. The distribution of the various chemical species within the solid and the solution phases is not trivial, such that the calculation of the scattering length density contrast $\Delta\rho$ as defined in the model cannot be easily derived from sample composition. Moreover, the initial scaling of the measurable intensity (when calculating the apparent thickness from transmission) implicitly uses the volume fractions of each component. Accordingly, one has to take into account the fact that all the parameters ($\Delta\rho$, φ and the intensity) are linked through sample composition and need to be crosschecked.

The porous scattering model has been used to probe the four possible models for chemical distribution of the species inside the pores: (model 1) only water, (model 2) water + electrolyte, (model 3) water + electrolyte + nitric acid, (model 4) water + nitric acid. The porous volume fraction φ has been calculated in each case (from known weight fraction and density of each component) and injected in the model as an input. A corresponding calculated scattering length density contrast ($\Delta\rho_{\text{calc}}$) has been obtained. From equation (26*b*), we determined the experimental electronic contrast ($\Delta\rho_{\text{X-rays}}$) from X-rays measurements. The values found for the sample of Fig. 5 are listed in Table 1. The comparison between calculated and experimental contrast allowed the rejection of unphysical assumptions and proved that the pores were only filled by water (model 1). The agreement obtained in model 4 could seem as good as that obtained with the model 1. Nevertheless, this is peculiar to this sample, and the average agreement when one slightly varies the initial content of $Al(NO_3)_3$ in the solution from 0 to 0.15 *M* is much better for model 1 than for model 4 (Lyonnard *et al.*, 2002). Nitric acid and electrolyte are located inside the matrix grains, or at the interface with the pores. The application of the scattering model in that case not only allowed the identification of quantities such as Σ_S, but also produced an important picture of the chemical organization inside the grains. The specific surface, and the size of the pores and of the grains were finally obtained as usual from equations (28) and (30), and compared with BET and SEM measurements, as listed in Table 2 for the sample of Fig. 5. The existence of a closed porosity in the powders has been derived from the discrepancy between BET and USAXS data (8% in the case of Table 2). Moreover, the comparison of the various samples allowed the variations of

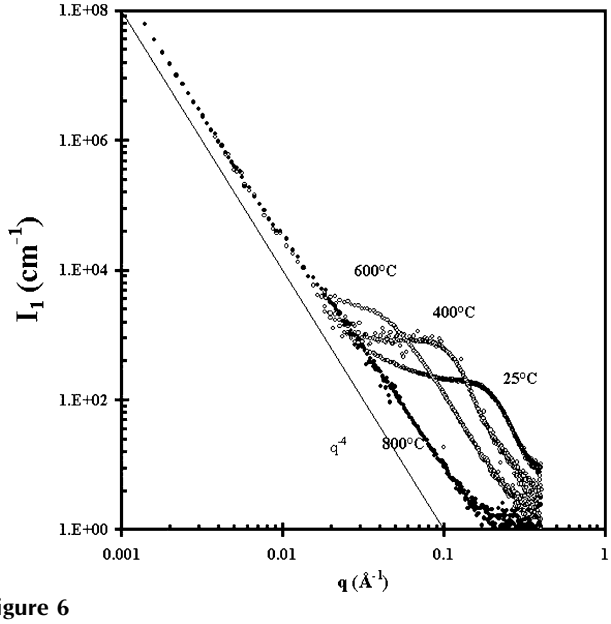

Figure 6
(U)SAXS spectra of glasses of CeO_2 obtained by slow evaporation of a colloidal suspension of CeO_2 particles. The glasses have been calcinated at different temperatures for 1.5 h.

Table 3
Physical parameters obtained from SAXS spectra for the ceria glass before and after calcination at different temperatures.

Σ_S is the total specific surface of the grain, φ the pore volume fraction, d the equivalent diameter of a pore, and BET the specific surface obtained in BET (when available).

	Σ_S ($m^2\ g^{-1}$)	φ	d (nm)	BET ($m^2\ g^{-1}$)
298 K	159	0.25	1.9	150
673 K	52	0.16	3.4	80
873 K	12	0.06	5.1	1
1073 K	0.9	<0.01	10	<1

porosity and morphology to be linked to the pre-aggregation process in the sols.

4.3. Mesoporous ceria powders

Mesoporous matrices made of inorganic materials are thought to present great capacities for ion adsorption from aqueous solution, due to the size of the pores. Depending on the polarizability of the materials, selective adsorption may also be attained in the future. The first step in this long-term project is to produce and characterize mesoporous materials of polarizable atom oxide, such as ZrO_2 or CeO_2.

As a potential material, a porous cerium oxide glass has been formed by slowly evaporating a colloidal suspension of cerium oxide particles. Nanometric ceria particles $[CeO_2(HNO_3)_{0.5}(H_2O)_4]$ can be obtained following the procedure described by Briois *et al.* (1993) and Nabavi *et al.* (1993). The wet powder can be redispersed in water to form a stable colloidal sol. The suspension was washed first with nitric acid and then with water to reach a final pH of 3. Finally, the evaporation was driven at room temperature over several days.

The resulting colloidal glass was milled to give a powder. The initial powder was seen to be highly porous, as shown in Fig. 6. Furthermore, the inner porosity of the resulting powdered glass can be modified by burning the powder at different temperatures. Indeed, the heating promotes diffusion of atoms in the solid. Fig. 6 shows the scattering intensities measured by SAXS and USAXS for the initial glass, and after burning at respectively 673, 873 and 1073 K during 1.5 h. The overlapping between the SAXS and USAXS data is excellent, despite the very low values of the apparent thicknesses (from 1 to 10 μm, as calculated from transmission measurements, which means that only one layer of grains has been measured).

Two Porod regions are clearly evidenced, except at the higher temperature. There is no variation of the first Porod regime for all the diagrams, which indicates that the average size of the micronic grain does not vary with temperature. On the contrary, the signal at large angles from the second Porod regime is strongly affected by the heating. When increasing temperature, two main modifications appear. First, the amplitude of the intensity in the Porod regime decreases, which shows that the specific surface reduces. Second, the transition from the plateau to the Porod regime is located at a lower angle, meaning that the pores are becoming bigger. Hence, a mechanism of pore coalescence is clearly evidenced. At this stage it cannot be concluded whether these structural rearrangements happen at a constant porous volume fraction or not. Indeed, it may be that the pores both fuse and diffuse to the surface where they simply disappear, hence decreasing the core porous volume. The full fitting of the scattering diagram will provide a clearer answer.

The spectra have been analysed using the model developed for the case (i), *i.e.* without any solvent in the pores and a density of 7 g cm^{-3} for CeO_2. An attempt has been made to take into account the hydration of Ce at the ambient temperature, and we have shown that the best agreement in data analysis as compared with BET measurements has been obtained without water in the pores. The model allowed us to follow the variation of the internal structure caused by the calcination of the sample. The results are summarized in Table 3. In particular, it is clearly seen that the porous volume fraction is decreasing with the temperature increase and we conclude that the pores both fuse and diffuse to the surface of the grain.

The specific surface decreases when increasing the temperature, and the size of the pores increases. Nevertheless, a compromise can be obtained at 873 K between a high specific surface and large pores in the media, to obtain a material which can adsorb ions.

5. Conclusions

The interpretation of X-ray scattering diagrams for porous and granular media is available at a quantitative level, only when it is known precisely which chemical elements are present in the beam. In that case, the absorption coefficient of the sample can be calculated and an equivalent solid thickness e_B or an equivalent grain (solid + inner pores) thickness e_H can be derived, which allow the application of the general theorems of X-ray scattering. The requirement on chemical composition may appear difficult *a priori* in some very complex systems, but we have shown that the porous specific surface and volume can indeed be measured for systems as complex as porous glasses and synthetic mixed ceramics.

References

Bale, H. D. & Schmidt, P. W. (1984). *Phys. Rev. Lett.* **53**, 596–599.
Briois, V., Williams, C. E., Dexpert, H., Villain, F., Cabane, B., Deneuve, F. & Magnier, C. (1993). *J. Mater. Sci.* **28**, 5019–5031.
Brumberger, H. (1965). Editor. *Small-Angle Scattering*. New York: Gordon and Breach.
Guinier, A. & Fournet, G. (1955). *Small Angle Scattering of X-rays*. New York: Wiley.
Lambard, J., Lesieur, P. & Zemb, T. (1992). *J. Phys. I Fr.* **2**, 1191–1213.
Lyonnard, S., Bartlett, J. R., Sizgek, E., Finnie, K. S., Zemb, T. & Woolfrey, J. L. (2002). *Langmuir*, **18**, 10386–10397.
Nabavi, M., Spalla, O. & Cabane, B. (1993). *J. Colloid Interface Sci.* **160**, 459–471.
Né, F., Grillo, I.,Taché, O. & Zemb, T. (2000). *J. Phys. IV Fr.* **10**, 403–413.

Porod, G. (1951). *Kolloid K.* **124**, 83–114.
Porod, G. (1982). In *Small Angle X-ray Scattering*, edited by O. Glatter & O. Kratky, pp. 17–51. New York: Academic Press.
Ringwood, A. E., Kesson, S. E., Reeve, K. D., Levins, D. M. & Ramm, E. J. (1988). In *Radioactive Waste Forms of the Future*, edited by W. Lutze & R. C. Ewing, pp. 233–334. Oxford: Elsevier.
Schaeffer, D. W., Brow, R. K., Olivier, B. J., Rieker, T., Beaucage, G., Hrubesh, L & Lin, J. S. (1995). In *Modern Aspects of Small-Angle Scattering*, edited by H. Brumberger, pp. 299–307, NATO ASI Series. Dordrecht: Kluwer Academic.
Sizgek, E., Bartlett, J. R., Woolfrey, J. L. & Vance, E. R. (1994). *Mater. Res. Soc. Symp.* **333**, 305–312.
Strobl, G. R. (1970). *Acta Cryst.* A**26**, 367–371.
Wong, P. Z. (1985). *Phys. Rev. B*, **32**, 7417–7424.
Zemb, T., Taché, O., Né, F. & Spalla, O. (2003). *Rev. Sci. Instrum.* In the press.